ELSEVIER

Contents lists available at ScienceDirect

Materials & Design

journal homepage: www.elsevier.com/locate/matdes



Strength and its variability in 3D printing of polymer composites with continuous fibers



M. Parker^{a,1}, N. Ezeokeke^{a,1}, R. Matsuzaki^b, D. Arola^{a,c,*}

- ^a Department of Materials Science and Engineering, University of Washington, Seattle, WA, USA
- ^b Department of Mechanical Engineering, Tokyo University of Science, Tokyo, Japan
- ^c Department of Mechanical Engineering, University of Washington, Seattle, WA, USA

HIGHLIGHTS

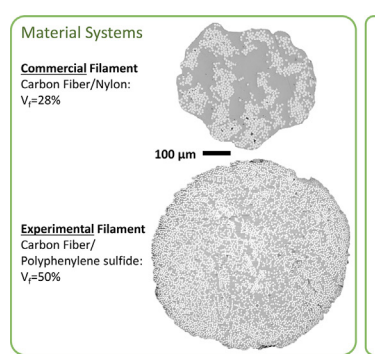
- Fused filament fabrication was performed on commercial and experimental filaments with continuous fibers.
- The strength of printed carbon fiber filament decreased from 10% to over 60%, with no correlation to fiber volume fraction.
- For the commercial filaments, those reinforced with Kevlar fibers underwent less degradation than with carbon fibers.
- Fibers near the filament surface incurred damage during printing that facilitates fiber fracture at extrusion.
- Damage to the filament and the reduction in reliability depends on material selection, process settings and hardware.

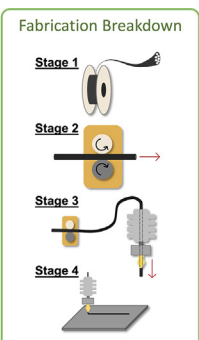
ARTICLE INFO

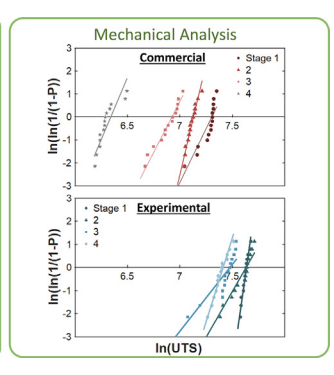
Article history:
Received 23 September 2022
Revised 26 November 2022
Accepted 13 December 2022
Available online 14 December 2022

Keywords: 3D printing Additive manufacturing Continuous fibers Strength Thermoplastic composites

G R A P H I C A L A B S T R A C T







ABSTRACT

Additive manufacturing (AM) of polymer composites with continuous fibers could play a major role in the future of aerospace and beyond but will require printed materials to achieve new levels of reliability. This study characterized the strength distribution of selected thermoplastic matrix composites as a function of printing via fused filament fabrication (FFF). Experimental and commercial composite filaments of continuous carbon or Kevlar fibers were printed with volume fraction (V_F) ranging from approximately 28 to 56 %. The strength was evaluated under uniaxial tension after specific stages of printing and Weibull statistics were applied to characterize the strength distribution. There was a significant reduction in strength of the printed material with respect to the unprinted condition, regardless of reinforcement type, fiber volume fraction or printer used. Damage introduced by feed extrusion of the filament, and fiber failures induced at material deposition were most detrimental. For carbon fiber filaments, the reduction ranged from approximately 10 % for an experimental material to over 60 % for a commercial filament. There was no correlation in the strength degradation or variability with V_F . The prevention of

Abbreviations: AM, Additive manufacturing; CCF, Continuous carbon fiber; FFF, Fused filament fabrication; PA, Polyamide; PPS, Polyphenylene sulfide; UTS, Ultimate tensile strength.

^{*} Corresponding author.

E-mail address: darola@uw.edu (D. Arola).

¹ contributed equally to this manuscript and share the first author role.

process-related fiber damage is key to advancing AM for continuous fiber composite and application to designs intended for stress-critical applications.

© 2022 The Authors. Published by Elsevier Ltd. This is an open access article under the CC BY-NC-ND license (http://creativecommons.org/licenses/by-nc-nd/4.0/).

1. Introduction

Additive manufacturing (AM) of composite materials is an area of incredible opportunity. The high strength-to-weight ratio of composites, combined with the various advantages of AM including light-weighting, nearly unlimited complexity, and low materials waste makes the prospects for advancing the design and performance of structures almost unlimited. Applications for AM of composites are envisioned from sea to sky, as well as in space exploration [1,2].

In comparison to the rapid advancements in AM of monolithic polymers and metals, the growth in 3D printing methods for fiber reinforced composites has been slow. In fact, a unique or "dedicated" method for printing composite materials is not available. Rather, techniques developed for specific classes of monolithic materials are typically adapted to accommodate materials with reinforcement. For instance, fused filament fabrication (FFF), a method traditionally used for printing of monolithic thermoplastics, is now commonly used for AM of composites [3]. The FFF process has become widespread and sought for the development of prototypes as well as the production of near-net and net-shape polymer components. Applied to composites, FFF can manufacture components without tooling and reduces the need for significant post-mold-processing, thereby overcoming drawbacks associated with thermoset matrices [4–6]. Admittedly, the FFF process is currently limited by speed and the size of printable structure. Nevertheless, it fulfills a particular niche in size and materials that other AM processes are unable to compete with.

In FFF, filaments with a thermoplastic matrix are heated above the melting temperature of the polymer, extruded through a nozzle, and deposited in a layer-by-layer process according to a computer aided design of the part geometry [4,7-9]. There are some challenges in FFF that are ubiquitous across materials, including the interior interlayer strength, the presence of voids in the printed components and the complications to developing new reliable filaments [4,10,11]. Regarding FFF with composite filaments, Brenken et al. [3] reviewed studies that explore printing materials with discontinuous and continuous fibers. One advantage of FFF with respect to other AM methods [12] is that short discontinuous fibers are aligned via extrusion, which enhances the material strength and stiffness [13,14]. FFF of composites with continuous fibers could yield superior strength to those with short fiber reinforcement due to the greater degree of shear coupling and loadcarrying borne by the reinforcement.

Tian et al. [15], recently reviewed the developments in 3D printing of continuous fiber composites and highlighted innovations in materials and structural designs. There are special challenges to FFF of continuous fiber composites including the need for intelligent tool path design, intrinsic limitations in the process capabilities [15], and unique printing-related defects [16]. Commercial printers have been developed for printing continuous fiber composites by FFF [9,11,13,17]. However, damage introduced during the printing process is concerning. Hu et al. [18] were first to quantify the strength degradation in FFF of a commercial filament of polyamide (PA) reinforced with continuous carbon fibers (CCF). They reported that the tensile strength of the printed filament was 60 % lower than that of the unprinted condition. Based on a methodical evaluation, the largest degree of damage was identified

in the final stage of printing, i.e., as the filament is deposited onto the printer bed or previous layer. While highly novel, this study was limited to one filament system and one commercial printer. Meanwhile, Zhang $et\ al.\ [19]$ examined the forces acting on the filament in printing of a CCF composite (V $_f$ = 27 %) in matrix of polylactic acid. They found that void formation, strength, surface quality and dimensional accuracy depended on a competition between the ironing and traction forces.

A limitation to most studies involving FFF of filaments with continuous fibers is their low fiber volume fraction ($V_f \leq 30$ %). However, a recent study reported success in FFF of experimental filaments consisting of continuous carbon fibers with higher V_f (30 to 50 %) [20]. Another effort involving pultrusion of a commingled carbon fiber/nylon fiber tow achieved volume fractions of 44–47 % [21]. These new composites for FFF with higher V_f could achieve superior levels of performance, provided that printing-related fiber damage can be overcome. Understanding the variables contributing to printing damage is key.

In this investigation, FFF of continuous fiber composites was conducted with both commercial and experimental filaments to evaluate process damage and degradation in the mechanical properties with respect to the filament structure and specific stages of the printing process. The primary objectives were to: i) characterize the strength and its variability in FFF of composite filaments with continuous fibers over an extended range of V_f, ii) compare results for printing commercial filaments with continuous fibers of carbon and Kevlar, and iii) identify the mechanisms of degradation contributing to the reduction in strength and reliability of these materials printed by FFF. With respect to previous studies in this area, the present investigation makes a fundamental contribution to understanding FFF of continuous fiber composites. It is the first to report on the mechanical properties achieved in printing filaments reaching 50 % V_f, to consider the importance of fiber type on printing-related damage and strength distribution, and to address whether the damage incurred during printing is printerand hardware-dependent. The results support an identification of the changes needed to reduce damage and increase material reliability, which will be key to optimizing the process and to enable scaling to produce composite structures with confidence.

2. Materials and methods

The principal material system used in this investigation consisted of prototype filaments for FFF produced by Toray (Toray Industries, Inc, Japan). These filaments contain a tow of aerospace grade continuous carbon fibers (CCF) embedded within a matrix of polyphenylene sulfide (PPS). Additional details regarding the fiber type and the grade of PPS are proprietary. Two different CCF/PPS filaments were included in this effort, which are denoted here as T-40 and T-50, according to their nominal $V_{\rm f}$ of 40 % and 50 %, respectively; their exact volume fractions estimated using image analysis are 43.5 % and 48.7 %. Both filaments consisted of a single tow of 6 k fibers and the same fiber type. The diameters of the T-40 and T-50filaments are 0.58 mm and 0.56 mm, respectively.

Two additional commercial material systems were also evaluated, including filaments of CCF and continuous Kevlar fibers, each within a PA matrix. The two systems were acquired from Markforged (Markforged, Inc, Watertown, MA, USA), and are referred

to here as MF-CF and MF-K, respectively. The MF-CF possesses a diameter of 0.4 mm and V_f of approximately 28 %, whereas the MF-K has a diameter equal to 0.34 mm and an estimated V_f of 56 %. These materials were utilized as a source of comparison to the experimental filaments produced by Toray and to provide broader understanding of relationships between the reinforcement and printing damage that ensues. Results obtained for the MF-CF served as a source of comparison with those in Hu *et al.* [18].

Two different printer systems were used for FFF. The first system consisted of a modified desktop printer (Prusa, Model I3 MK3S, Prague, Czech Republic). Specific modifications include replacement of the metal rollers of the extruder assembly with a polyurethane drive roller, a secondary rubber roller and installation of polytetrafluoroethylene (PTFE) tubing to guide the filament from the extruder rollers to the nozzle assembly (Bowden assembly). A brass nozzle with a 1.2 mm diameter was implemented. The appropriate conditions for printing of the experimental CCF/ PPS were described in previous work [20], along with a detailed description of the printer modifications. The Prusa printer was used to print all four filaments, including the T-40, T-50, MF-CF and MF-K. Printing of the CCF/PPS was conducted using a nozzle temp of 340 °C and with a layer height of 0.2 mm. The MF-CF and MF-K filaments were printed with the Prusa system at 250 °C and 270 °C, respectively, and with a layer height of 0.2 mm to maintain consistency. All filaments were extruded at a rate equal to the feed rate to preclude clogging or breakage of the filament. In addition to the modified Prusa printer, a commercial Mark Two 3D printer was used (Markforged, Inc, Watertown, MA, USA). The latter was used for printing the MF-CF and MF-K filaments only due to restrictions of the warranty. The system is supplied with a 0.9 mm diameter brass nozzle for continuous fiber extrusion. The layer height used for printing with the Mark Two printer was adjusted as necessary for the individual filaments.

Damage to the filament that resulted from printing was of primary interest in this investigation, as well as the reduction in strength with respect to the unprinted, or "as-received" condition. To understand the progression of filament damage as it undergoes printing, the material flow within the Prusa printer was divided into four stages including: i) the as-received condition (Stage 1); ii) after passing through the extruder rollers but prior to heating (Stage 2); iii) after passing through the extruder rollers and the heated nozzle (Stage 3); after completing the previous stages and being deposited onto the heated print bed (Stage 4). These stages were adopted from the recent investigation of Hu et al. [18] in printing MF-CF via FFF and are applied here for consistency. Due to restrictions of the Markforged warranty, it was not possible to intervene during printing and extract portions of the filament from Stage 2 and Stage 3. Therefore, printing with the Mark Two was restricted to Stage 1 and Stage 4. The printers and a breakdown of the individual stages of printing are depicted in Fig. 1.

To understand contributions of processing to damage, the microstructure of the filaments was evaluated in the as-received (unprinted) and printed condition. Sections of each filament were mounted in a two-part epoxy and polished according to a traditional process involving silicon carbide abrasive papers from mesh number #800 to #4000, followed by final polishing accomplished with felt pad and alumina particle suspensions with particle size from 3 to 0.3 μ m. Optical microscopy was performed with an Olympus Model BX51M (Olympus Corporation, Center Valley, PA, USA) and an Olympus SC30 camera (1024 \times 768 resolution). Scanning electron microscopy (SEM) of selected samples was conducted before and after mechanical testing using a Phillips Model XL30 (Philips/FEI Company, Lausanne, Switzerland). The samples were sputtered with a 4 nm layer of platinum and imaged at a beam accelerating voltage of 5 kV.

Sections of filaments were printed with length of approximately 400 mm using the Markforged and Prusa printers to enable

mechanical testing. While the Mark Two is capable of printing sections of that length, the Prusa printer is limited to approximately 250 mm. To print longer lengths, two Prusa printers were placed in series, and a steel print bed spanned the total distance of the two printers. The second printer allowed for longer controlled movements of the new print bed, which extended past its original position and enabled uniaxial testing of printed samples to be directly compared to the other printing stages.

Tensile testing was performed on axial sections of each filament for the four different stages. For Stage 1, samples were cut directly from the spool. Stage 2 and 3 samples were only prepared using the Prusa printer. For Stage 2, the filaments were run through the extruder rollers and then cut to length. For Stage 3, the base of the print bed was removed to enable the filament to be extruded in continuous vertical sections from the nozzle. In Stage 4, all samples on the Prusa printer were printed on a steel bed. On the Mark Two. Stage 4 samples were printed at conditions prescribed by the Eiger software settings for the respective filaments (i.e., MF-CF: 255 °C and 0.125 mm layer height; MF-K: 260 °C and 0.1 mm layer height). The Eiger software of the Markforged printer requires that the printing of the filament with continuous fibers is performed on top of a previous layer of Onyx or neat polyamide. To achieve a section of printed CCF that is isolated from other layers, a rectangular base layer of onyx was printed, and then a layer of masking tape was placed over the top. A single contour of the chosen reinforced filament was then printed on top of the masking tape. That process enabled the printed filament with continuous fibers to be lifted from the tape with ease and ensured that testing of the printed filament did not involve extra material or damage introduced by separation.

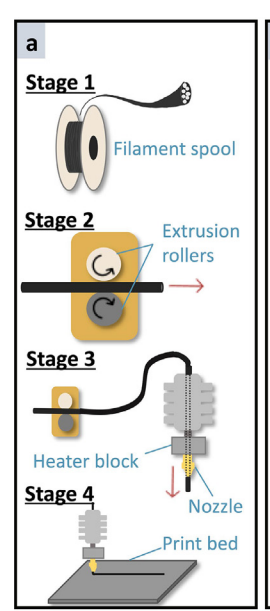
Tensile testing of the filaments was performed using a commercial universal testing frame (Model E1000, Instron Corporation, Norwood, MA, USA) that was equipped with a set of specialized fixtures for axial testing of filaments [20]. The sample ends were sandwiched between sandpaper and an aluminum plate, which was clamped to the fixtures via a small metal C-clamp. Loading was conducted in displacement control at a rate of 1 mm/min, resulting in a strain rate of approximately 0.01 s⁻¹. The instantaneous load and displacement were acquired continuously at a rate of 5 kHz. The engineering stress was estimated according to the cross-sectional area, which was calculated from an average of 3 measurements taken within the gauge section over approximately a 90 mm length. The measurements consisted of diameters for Stages 1 through 3 and width and thickness for Stage 4. The ultimate tensile strength (UTS) was obtained from the maximum load and average cross-section area. Only samples that failed within the gauge length were considered valid and results from other failures were discarded. There was no correlation in specimen failure characteristics based on specimen or printer type. A total of n = 15 samples were successfully tested for each stage of printing with each of the printer systems, resulting in 270 samples in total. The average and standard deviation of the UTS for each stage and material were obtained. Furthermore, a repeated measures t-test was utilized to compare the strength of the samples across the printing stages. Significance was defined by $p \leq 0.05$. A two-parameter Weibull analysis was performed with the strengths according to:

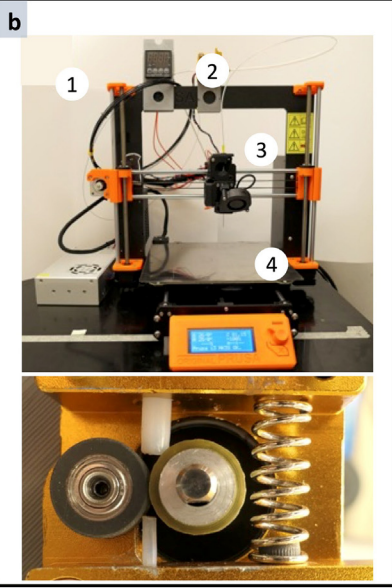
$$P(\sigma) = 1 - exp\left(-\left(\frac{\sigma}{\sigma_{\circ}}\right)\right)^{m} \tag{1}$$

where $P(\sigma)$ represents the probability of failure at the axial stress (σ) , m is the Weibull modulus, and σ_0 is the characteristic strength. The probability function for failure (P_f) was defined according to:

$$P_f = \ln(\ln(\frac{1}{1-P})) \tag{2}$$

where P was defined using the median rank according to





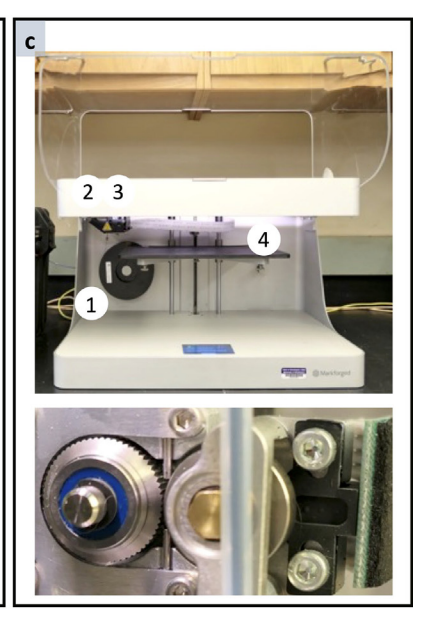


Fig. 1. Overview of utilized desktop printers. (a) Diagram of isolated printing stages for (b) altered Prusa I3 MK3S+ (top) with mounted rubber-wheeled extruder (bottom) and (c) commercial Markforged Mark Two printer (top) with dual metal extruders (bottom).

$$Median \, Rank = P = \frac{Stress \, Rank - 0.3}{Number \, of \, Samples - 0.4} \tag{3}$$

The Weibull parameters were obtained for each material and printer, and for each of the individual stages of material advancement (1 to 4) that were explored. A comparison of the Weibull parameters was performed to better understand the distribution in strength and contributions to its variability.

3. Results

The microstructure of the filaments in the as-received condition (i.e., Stage 1) is shown in Fig. 2. As evident from this figure, the fibers in the MF-CF and MF-K filaments shown in Fig. 2a and 2b, respectively, are less uniformly distributed than those in the T-40 and T-50 filaments in Fig. 2c and 2d. The filament with the most uniform fiber distribution and volume fraction is the T-50 filament. In general, the filaments with lower nominal fiber volume fraction (i.e., MF-CF and T-40) exhibit isolated regions that are matrix rich.

The microstructure of selected filaments after printing (i.e., Stage 4) is shown in Fig. 3. Due to ironing of the heated filament by the nozzle onto the print bed, printing transforms the filament from a circular cross section in the as-received condition to roughly a rectangular cross-section. Based on the microstructure analysis, both systems have a void content less than 2 %. Furthermore, there was no damage evident in the individual fibers from this perspective of the analysis. Of the two printed filaments shown in Fig. 3, the T-50 (Fig. 3b) exhibits the most uniform distribution of carbon fibers after printing. Nevertheless, it is important to note that it does have a rougher top surface as a result of peripheral fibers.

Results for the average UTS of the four filament systems are shown in Fig. 4 and correspond to the stages of material advancement through the printer. Specifically, Fig. 4a presents results for the T-40 and T-50 filaments printed on the Prusa printer. These two filaments exhibited an average UTS in Stage 1 (unprinted) of 1845 ± 175 MPa and 2035 ± 70 MPa, respectively. There is a decrease in strength that occurs to both filaments from Stage 1 to 4 as evident from the distributions. The T-50 underwent a significant decrease in strength in Stages 3 and 4 with respect to Stage 1. The T-40 also underwent a reduction in UTS, with significant

reduction at all stages with respect to Stage 1. However, the incremental reductions in strength for the T-40 from Stages 2 to 4 were not significantly different. For the T-50 filament, the incremental reduction in strength was only significant from Stage 2 to 3. A detailed analysis of the statistical measures can be found in Table S1-S4 of the Supplemental Information (SI).

Results for the MF-CF and MF-K filaments are presented in Fig. 4b and 4c, respectively. The average UTS of the MF-CF and MF-K filaments in Stage 1 (unprinted) are 1410 ± 150 MPa and 875 ± 40 MPa, respectively. Consistent with the responses in Fig. 4a, there is a degradation in strength with progressive stages of the printing process. Most notable for the MF-CF filament, there is a significant reduction in the UTS for each incremental stage of material advancement. For the MF-K filament the incremental reduction in strength is only significant for Stages 2 to 3 and 3 to 4. Also evident in Fig. 4, the UTS was significantly lower for the filaments processed using the Markforged printer relative to the Prusa system. Hence, there are contributions from the hardware to the degree of degradation and reduction in strength.

A summary of the strength measurements for each stage is presented in Table 1, along with estimates for the total degradation that accumulated from Stage 1 to Stage 4. These results are categorized in terms of the material, printer, and the individual stages of the process. A comparison of the values in this manner shows that all filaments underwent a reduction in strength over the four stages of printing and that the overall degradation in strength from Stage 1 to Stage 4 ranged from $\approx\!10\,\%$ to over 60 %. For instance, the T-50 underwent a 5 % and 20 % loss after Stages 2 and 3 with respect to the unprinted condition (Stage 1), and a total reduction of 21 % after Stage 4. In contrast, the T-40 filament underwent an 8 % reduction in strength from Stage 1 to Stage 2 but did not undergo further degradation through Stage 3 and Stage 4; the total reduction in strength of the T-40 filament after Stage 4 was 8 %. As evident from the summary of degradation estimates in Table 1, the experimental CCF/PPS filaments underwent less degradation in strength with respect to the unprinted condition than the commercial filaments.

Analogous to the T-40 and T-50, the MF-CF and MF-K filaments underwent a decrease in strength after each stage of printing with the Prusa printer (Table 1). The largest reduction occurred to the

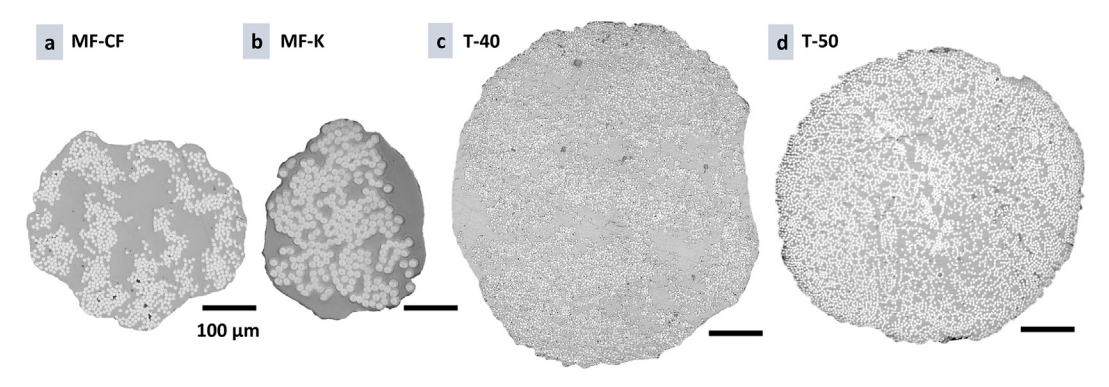


Fig. 2. As-received microstructure for (a) MF-CF, (b) MF-K, (c) T-40, (d) T-50, noting the higher void percentage in MF-CF and the differing individual fiber radii between Markforged and Toray.

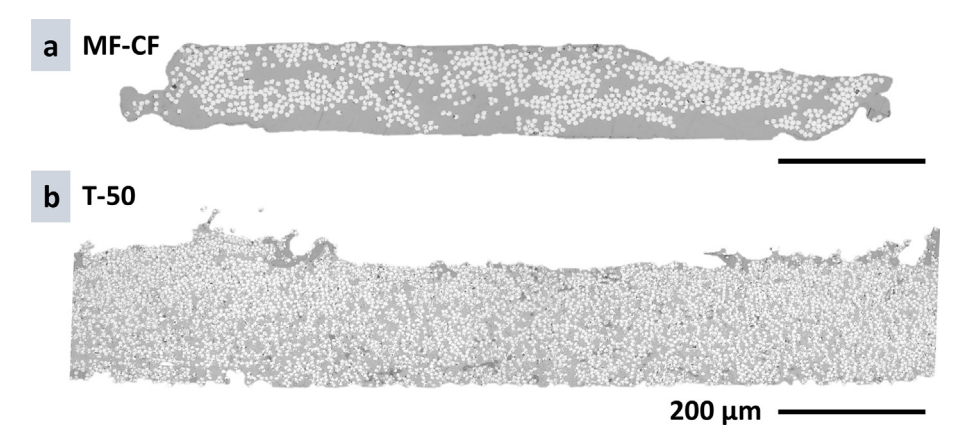


Fig. 3. Printed microstructure for (a) MF-CF and (b) T-50 where the bottom of the micrograph was the surface in contact with the heated print bed.

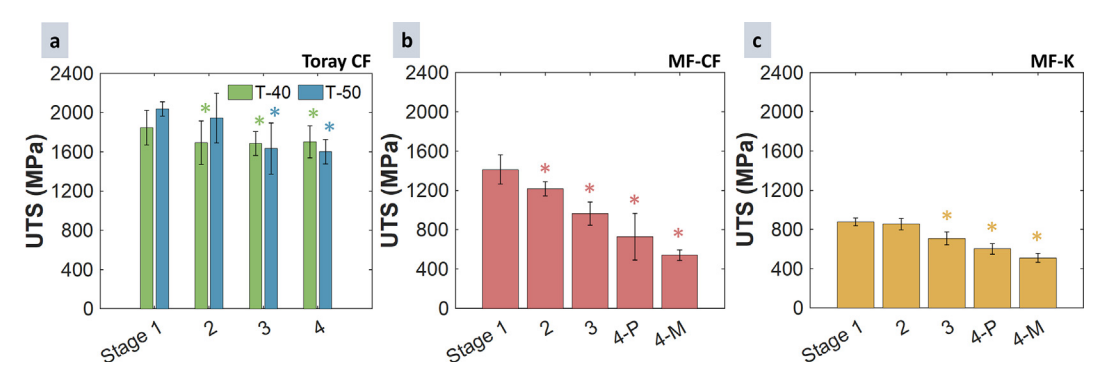


Fig. 4. Comparison of uniaxial ultimate tensile strength between filaments as a function of the isolated printing steps for a) T-40 and T-50 tested on the Prusa MK3S+, b) MF-CF, and c) MF-K. 4-P and 4-M denote if the samples were printed on the Prusa or Markforged printers, respectively. * Denotes significance (p-value less than 0.05) from asreceived condition.

 Table 1

 Average ultimate tensile strength along with standard deviation for each filament, including total strength reduction from the as-received condition.

| Material/ Printer | MF – Carbon Fiber | | MF – Kevlar Fiber | | Toray – Carbon Fiber | |
|--------------------|-------------------|------------|-------------------|----------|----------------------|------------|
| | Prusa | MF | Prusa | MF | T40 | T50 |
| Stage 1 | 1410 ± 150 | 1410 ± 150 | 875 ± 40 | 875 ± 40 | 1845 ± 175 | 2035 ± 70 |
| Stage 2 | 1215 ± 70 | _ | 855 ± 60 | _ | 1690 ± 220 | 1940 ± 250 |
| Stage 3 | 960 ± 120 | _ | 710 ± 65 | _ | 1685 ± 120 | 1630 ± 260 |
| Stage 4 & | 725 ± 240 | 540 ± 55 | 600 ± 55 | 510 ± 45 | 1700 ± 165 | 1600 ± 125 |
| Strength Reduction | 48 % ↓ | 62 % ↓ | 31 % ↓ | 42 % ↓ | 8 % ↓ | 21 % ↓ |

filament with carbon reinforcement and after Stage 4, for a total reduction of nearly 50 %. For the Kevlar filament the degradation

in printed strength was lower but exceeded 30 %. Interestingly, the degradation in strength of the MF-CF and MF-K materials

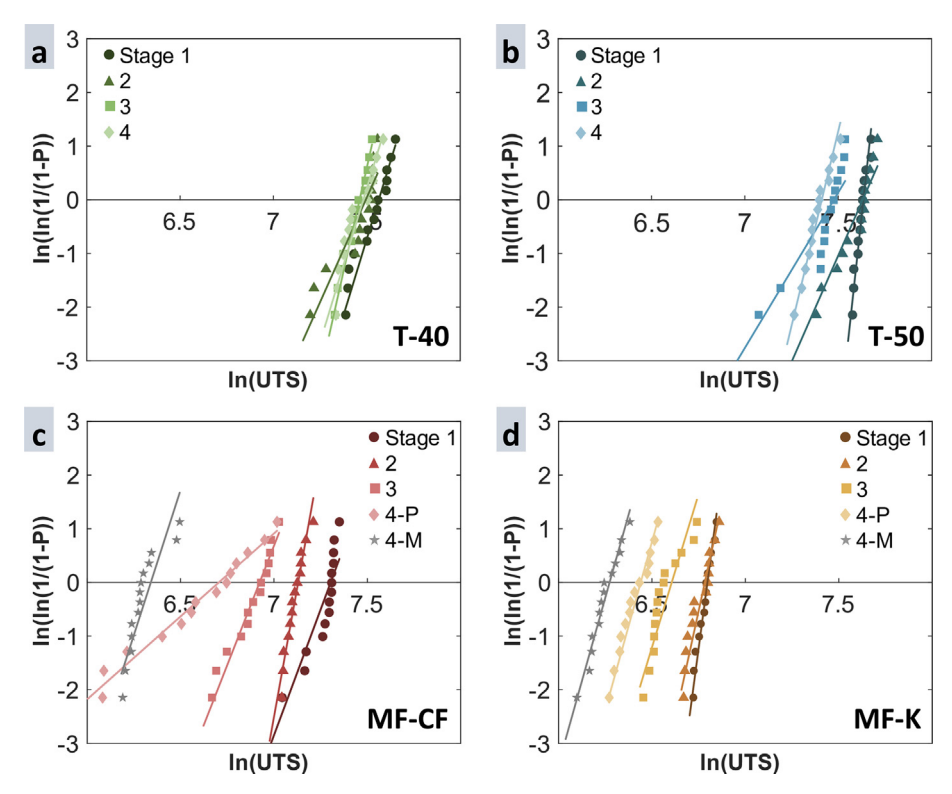


Fig. 5. 2-parameter Weibull analysis for the printing stages investigated of each filament system where a higher slope with a closely linear fit denotes a higher material reliability with single failure mode.

was more extensive when printed with the Mark Two printer, by approximately 100–200 MPa, or roughly 10 %. Indeed, the MF-CF and MF-K fiber filaments underwent total reductions (from Stage 1 to 4) of 62 % and 42 %, respectively, after printing on the commercial printer. Although the lowest standard deviation in strength of the two commercial filaments was exhibited by the Kevlar fiber filament, regardless of the printer used, the coefficient of variation in strength for the Carbon and Kevlar fiber filaments were approximately equal, with average of approximately 10 %.

The Weibull distributions for the estimated UTS are presented in Fig. 5 as a function of the stage and printer utilized. The corresponding Weibull moduli associated with the strength distributions are presented in Table 2. Fig. 5a and 5b show the Weibull distributions for the T-40 and T-50 filaments, respectively. Both filaments undergo a large reduction in Weibull modulus and characteristic strength in Stage 2 with respect to the unprinted condition, which signifies a reduction in strength and an increase in its variability. Comparing the T-40 and T-50 responses, the reduction in strength with advancement through the stages is greater for the T-50 material, which is evident from the greater translation leftward in the distributions in Fig. 5b. The degree of variability associated with each stage is comparable apart from T-50 in the asreceived condition. That filament exhibited the highest Weibull modulus (32.1) in Stage 1 but underwent a substantial decrease after passing through the extruder and nozzle in subsequent stages.

Table 2Reported Weibull modulus for each filament grouping.

| materials | MF-CF | MF-K | T-40 | T-50 |
|-----------|-------|------|------|------|
| Stage 1 | 9.4 | 26.1 | 11.4 | 32.1 |
| Stage 2 | 19.4 | 16 | 7.8 | 7.9 |
| Stage 3 | 8.9 | 11.5 | 15.5 | 5.8 |
| Stage 4-P | 3.1 | 12.6 | 11.5 | 14.5 |
| Stage 4-M | 10.8 | 12.4 | | |
| | | | | |

Fig. 5c and 5d present the results corresponding to the four stages of printing with the Prusa printer, as well as for Stage 4 with the MF printer, for the MK-CF and MK-K, respectively. There is a clear reduction in strength and increase in variability that results from advancement of the filament through the various stages of printing. In general, the largest modulus occurs in the asreceived condition, signifying the least variability, and decreases with advancement of the filament through the stages of printing, excluding Stage 2 (extruder only). Although the samples printed with the Prusa system have a larger degree of variability in UTS, the average strength exceeds that obtained for material printed with the Mark 2. Interestingly, the strength distribution for the MF-K filament exhibits the highest modulus (m = 26.1) of the commercial filaments in the unprinted condition. Nevertheless, there is a consistent decrease in Weibull modulus to roughly 12 for the printed MF-K samples obtained from both the Prusa and Mark 2 systems, which signifies an increase in the variability of printed strength.

A combination of optical microcopy and scanning electron microscopy (SEM) were used to inspect the filaments for damage introduced during the various stages of printing. Fig. 6 shows images obtained from optical microscopy of the T-50. Similar images for the MF-CF can be seen in Fig S1 in the SI. In general, there was no difference in the characteristics of these two filaments as they passed through the various stages of printing. In the as-received condition, the filaments exhibited smooth surfaces with no apparent defects. After Stage 2 and 3 some broken fibers and/or bundles of fibers are evident on the surface of the filament, as highlighted for the T-50 in Fig. 6b and 6c. Fiber waviness is evident on the macroscale in Fig. 6d, resulting in several bundles of fibers that have been separated from the main body. There are also areas on the surface with less matrix coverage or where it has been completely removed.

Fig. 7 presents SEM images of the T-50 filament taken at various stages of material advancement and with concentration on the

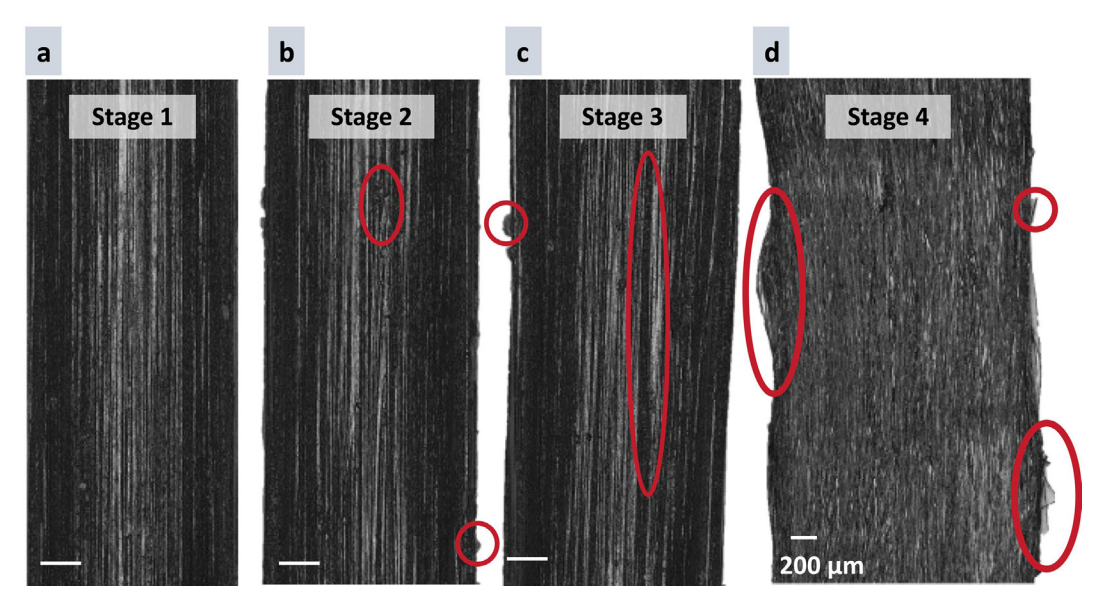


Fig. 6. Optical microscopy T-50 through all stages, noting increase in surface defects as the filament passes through the system.

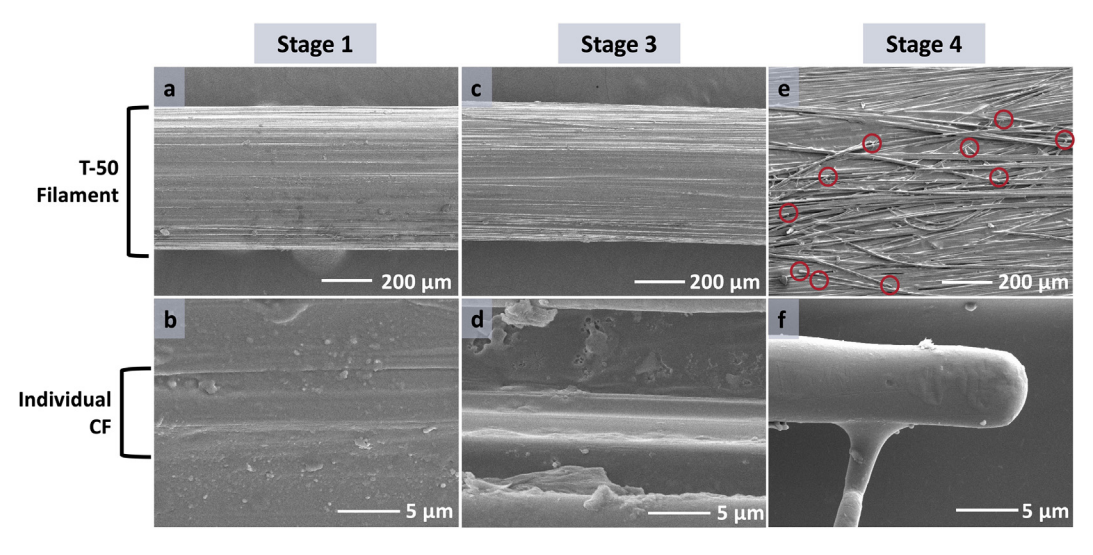


Fig. 7. SEM Images of T-50 at (a,b) Stage 1 showing fibers completely covered in PPS matrix, (c,d) Stage 3 where the matrix has been sheared off exposing fibers, and (e,f) Stage 4 where individual and fiber bundles are fully broken and exposed.

peripheral fibers. In Stage 1 (Fig. 7a-b) there is no evidence of surface damage, and the PPS matrix appears intact. At Stage 3 (Fig. 7c-d) there is evidence that the matrix has been disrupted, exposing carbon fibers near the surface. Damage becomes more evident at Stage 4 (Fig. 7e-f) where fibers are uncovered and have undergone fracture. An isolated broken carbon fiber is shown in Fig. 7f, which is still secured to the filament by the PPS matrix. The PPS appears to have encased the fractured fiber while the matrix was heated. These observations highlight fiber damage within the printed filament, that undoubtedly contribute to the reduction in tensile strength.

4. Discussion

The tensile strength of the experimental filaments with continuous carbon fibers exceeds the values previously reported for filaments with discontinuous and continuous fibers [3,4]. Specifically,

the average UTS of the experimental T-50 filament in the Stage 1 condition surpassed 2 GPa, which is significantly greater than that for other printable materials with high specific strength, including aerospace grade aluminum alloys (e.g. [22,23]) and even some titanium alloys (e.g. [24,25]). This is an exciting opportunity for AM of fiber reinforced composites and could set the stage for numerous applications - provided that the strength after printing is comparable to that before printing and with limited variation.

The UTS of the MF-CF filament for the four stages of printing were presented in Table 1. Comparing these results to those recently reported by Hu *et al.* [18] shows that the measured strengths of the filaments are in very good agreement across the four stages. For the MF-CF processed using the Markforged printer, the average UTS estimated for Stage 1 and 4 from the present study are 1410 MPa and 540 MPa, respectively (Table 1). For the same material and printer, Hu *et al.* [18] reported strengths for Stages 1 and 4 of roughly 1490 and 600 MPa, respectively. Both studies observed a reduction in the UTS from Stage 1 to Stage 4 of approx-

imately 60 %. The best stage of printing to compare results across these two studies is Stage 1 as it excludes potential printerspecific contributions to the UTS. Indeed, these values are within 5 %, which provides confidence in the reported strengths and methodology. In comparing the results for Stage 4, the strengths are within 10 %, which is an acceptable degree of variation considering that the differences can be printer dependent. Although printer-specific variability in mechanical properties is a topic of substantial industrial relevance, it has not been explored in AM of composites to date.

Results obtained for printing of the MF-CF on the Prusa printer exhibit a similar trend, with reduction in UTS from Stage 1 to Stage 4 of 1410 to 725 MPa. Although the decrease in UTS reached nearly 50 %, it is at least 10 % lower than that resulting from the same filament printed with the Markforged printer. There are three potential sources for the lower degradation, namely the differences in extruder hardware, nozzle diameter and laver offset. The extruder in the Prusa printer was modified to a Bowden configuration with rubber roller replacing the cogged steel drive roller. That modification reduced damage to the peripheral fibers of the filament and tempered the reduction in UTS at Stage 2 in comparison to that in Hu et al. [18] (14 % vs 20 %). Minimizing damage to the filament in extrusion is essential to reduce degradation and variability in subsequent stages. As the filament advanced, the reduction in UTS increased to 32 %, and then 48 % for Stage 3 and 4. Of note, a larger nozzle was used in the Prusa printer (1.2 vs 0.9 mm diameter), which could decrease the degree of restraint to fiber movement in the nozzle and fiber abrasion (i.e. components of damage). The difference in nozzle size was necessary to accommodate the larger filament diameter of the T-40 and T-50. In addition, a larger layer offset (0.2 mm) was used with the Prusa compared to the Markforged printer (0.15 mm). An offset of 0.15 mm is the set height for MF printers and cannot be changed. The larger offset used with the Prusa would reduce the ironing force and is expected to decrease scraping and damage of the near-surface fibers in Stage 4. Clearly, the printer hardware and process parameters can contribute to filament damage. Here, their effects appear to be confounding and further systematic study is necessary to understand the specific conditions necessary for minimizing damage.

Across the four different filaments printed, the reduction in strength in Stage 2 with respect to the unprinted condition ranged between 2 and 14 %. Indeed, the fibers are subject to concentrated contact induced via the pinch force of the extruder rollers. In printing with the Mark Two system, Hu et al. hypothesized that elongated abrasions during this stage are caused by the teeth of the metal extrusion rollers that bite into the matrix [18]. Indeed, replacing the metal rollers in the Prusa with more compliant polymers appeared to reduce the damage and degree of strength reduction (Table 1). In fact, there was no significant reduction in strength (P > 0.05) between Stage 1 and 2 for the T-50 and MF-K materials printed with the Prusa system. Admittedly, the T-40 did exhibit a reduction in strength at Stage 2, despite the roller upgrades. That variability could be attributed to disparities in quality associated with production of small batches of the experimental material (for the T-40 and T-50) or a reflection of inconsistencies in samples extrusion. Also of note, the T-40 filament was slightly more irregularly shaped (Fig. 2), which could manifest into a higher degree of variation in Stage 2 printing damage and subsequent mechanical behavior.

The filament undergoes rolling contact in Stage 2, which is expected to impart surface and sub-surface damage. Although the SEM analysis of filaments from Stage 2 did not reveal surface damage or disruption to the near-surface fibers, there was a reduction in strength (Table 1). The largest decrease in UTS for Stage 2 reached 14 % and occurred to the MF-CF filament. The least degradation occurred to the MF-K filament, which is expected from the

lower hardness and corresponding great damage tolerance of Kevlar fibers relative to carbon. The T-40 and T-50 filaments also appeared more resilient to Stage 2 damage than the MF-CF. One contribution is believed to be from the 6k fiber tow in the T-40 and T-50, in comparison to the 1k tow in the MF-CF. The higher fiber count reduces the percentage of damaged fibers relative to those not damaged within the core, moderating the decrease in strength for the T-40 and T-50. Considering the percentage of load carried by each fiber in the two filament systems, the MF filament only requires one sixth of the extent of fiber damage to suffer the same percentage reduction in strength as the Toray filaments. Yet, another potential factor is the shape of the filaments. Fig. 2a demonstrates that the MF-CF has the most irregular shape, along with the highest percentage of fibers near the surface. This combination could lead to more aggressive abrasion of fibers and more substantial reduction in tensile strength.

Details from the microscopic analysis in Fig. 7 showed that Stage 3 caused significant changes to the matrix and fibers near the surface of the filament. During this stage the matrix transitions from solid to liquid within the nozzle and the reduction in viscosity enables the fibers to migrate towards the surface. With advancement through the nozzle, exposed fibers can undergo sliding contact with the nozzle interior and accumulate damage. Indeed, by analyzing individual fibers Hu et al. determined that flaws introduced to the surface of the fibers contributed to the reduction in printed strength [18]. According to the Weibull distribution (Fig. 5) the filaments underwent a reduction in UTS in Stage 3 and an increase in strength variability. With exception of the T-40 filament, the Weibull modulus decreased substantially in Stage 3 (Table 2), which suggests that damage to the fibers occurred, but that it was inconsistent among the samples evaluated. Comparing the commercial and experimental filament groups, the reduction in Weibull moduli for the T-40 and T-50 are less severe. That could suggest that the PPS matrix is more effective in preventing damage in Stage 3 and highlights the potential material dependence in the strength distribution.

In Stage 4 the filament exits the nozzle and undergoes deposition. By virtue of the curvature, a tensile bending stress is imposed on peripheral fibers of the leading edge. Conversely, fibers on the trailing edge are in contact with the nozzle rim and experience a superposition of contact stress and compressive bending. As such, contact damage introduced to the filament in Stage 2 or Stage 3 could serve as the root cause for a reduction in strength of printed material in Stage 4. Of the two experimental filaments, the T-40 underwent the least degradation of strength in Stage 4. The T-50 filament with larger fiber volume fraction has fibers that are more exposed near the surface and susceptible to damage. The crosssections of printed filament (Fig. 3b) show that fibers at the surface were in contact with the nozzle during deposition. Therefore, it appears that the higher matrix content of the T-40 improves printability [20], as well as protects the fibers from damage in Stages 2 and 3, that could facilitate failures in Stage 4. That observation suggests there is potential for producing filaments with fiber V_f to obtain optimal printed strength and minimal fiber damage. Admittedly, this comment is speculative and the difference in volume fraction of matrix in the T-40 and T-50 filaments is not large. Clearly, additional study is necessary to confirm this interpretation.

There are many factors that can contribute to the Weibull modulus of strength distributions, such as gauge length, testing conditions, etc. that complicate comparisons across studies [26,27]. Nevertheless, the Weibull parameters for the filament strength distributions can be compared with those reported for other relevant materials. In general, a larger Weibull modulus signifies greater consistency in the strength measurement and is reflected by higher relative slope [20,28]. Hu *et al.*, [18] reported a Weibull modulus for individual carbon fibers of the MF filament in Stages 1 and 4

of 6.8 and 2.7, respectively. Overall, the estimated Weibull moduli for the fibers agree with those from other representative studies concerning single carbon fibers (5 to 8) [26,29,30]. The decrease in modulus from Stage 1 to 4 herein reflects an increase in variability resulting from the accumulation of damage with printing and different flaw types introduced across the four stages. A similar finding is found in the MF-CF filament, with Weibull modulus decreasing from 9.4 to 3.1 in printing from Stage 1 to Stage 4-P. One interesting characteristic of the strength distribution for the MF-CF system is the distinct bimodal quality evident for the filament in Stage 1 (Fig. 5c). This quality in the unprinted condition suggests that there is more than one family of flaw types and/or sizes that contribute to failure, which is concerning from a quality control standpoint. Intrinsic defects resulting in lower strength in the unprinted condition could only become exacerbated during printing.

Considering filaments, the low Weibull modulus of the MF-CF filament (m = 3.1) signifies the lower consistency in strength relative to the experimental carbon fiber filaments (m_{avg} = 13). As such, the experimental filaments appear capable of producing components with greater reliability. Remarkably, the T-50 had a modulus of 32.1 in Stage 1 but decreased to 14.5 in Stage 4. For comparison, the Weibull modulus of dry unidirectional CF tape lies between 23 and 39 [27]. Aerospace titanium and aluminum alloys can achieve Weibull moduli in strength of 20 and greater, which will serve as a benchmark for FFF of continuous fiber composites in the aerospace industry [31–33]. Although the experimental Toray filaments exhibit an impressive strength and comparatively high reliability, they are not immune to the undesirable decrease in strength and reliability after printing.

Since the T-40 and T-50 could only be printed with the Prusa printer, it is not possible to comment on the printer-dependent strength reductions of the experimental filaments. However, the MF-CF and MF-K filaments were printed with the two printers, and both exhibited at least 20 % greater strength when processed with the Prusa. The primary difference in the two systems were the modifications made to the extruder to reduce filament damage in Stage 2 and the slightly larger nozzle diameter (1.2 vs 0.9 mm). While the contributions to printed strength were distinct, the printer-dependent contributions to its variability is more difficult to address. In general, all the printed samples exhibit a unimodal Weibull response in Stage 4, signifying a single dominant family of flaws. But a single origin of failure was not identified in fractographic evaluations, suggesting that failure resulted from multiple defects accrued during printing as opposed to damage of individual fibers. In that regard the printers were the same, as there was no difference in the contribution of the printers to characteristics of failure. According to the Weibull moduli, there was essentially no difference in the degree of variability for the MF-K filament based on printer; $m \approx 12.5$ for both. In contrast, the variability in strength for the MF-CF filament was substantially greater when printed with the Prusa printer. The difference for these two materials is expected based on the greater flaw sensitivity of the carbon fibers in general and less uniformity in filament damage with improvements to the extruder. Both printers introduced damage to the filaments that caused a reduction in strength and increase in variability overall. Clearly, further improvements to printer hardware are needed.

Fiber orientation, infill pattern, as well as void characteristics contribute to variability in the strength of composites printed by FFF [34–37]. In comparison, there has been relatively limited recognition that fiber damage occurs in FFF and could cause a significant reduction in the strength of printed components. Based on the results for the four filaments and two printers, there is a universal reduction in the UTS of continuous fiber filaments printed using FFF. To be utilized for stress-critical applications, the damage

introduced to the material during FFF must be minimized. The reduction in properties with individual stages shows that solutions to reduce the extent of degradation and increase the reliability will likely require improvements to the material and the printer hardware.

Evaluating the mechanical properties of the filaments after various stages of printing provided quantitative estimates for the reduction in strength that could be correlated with the prevalent mechanisms. Dissecting the printing process into discrete stages also enabled an identification of sequential contributions to the total degradation. The novelty of the present study involved inclusion of multiple filament types and printers, which was key to understanding the material and process-dependence in the extent of damage incurred. That is a significant contribution. Despite the importance of this new understanding to advancing FFF of continuous fiber composites, there are multiple limitations to the present investigation that should be considered. Only single layers of the filaments were printed and evaluated in the present study. Components developed by AM in general can consist of hundreds of layers that are deposited on top of one another. In continuous fiber printing, the layer interfaces are parallel to the fiber direction, which results in absence of fiber reinforcement in the transverse direction. That topic has been evaluated recently in FFF of the T-50 material [38]. There are many additional struggles with multilayer printing of continuous fiber filaments, including void distribution, layer adhesion, controlling fiber/matrix distribution and path planning to limit fiber bundle overlaps. Hence, further investigation concerning FFF of continuous fiber filaments is necessary to advance the technology readiness level and capitalize on the opportunities ahead.

5. Conclusions

Fused filament fabrication (FFF) of thermoplastic polymer composites was conducted with commercial and experimental filaments consisting of continuous carbon and Kevlar fibers. The filament strength and primary contributions to its variability were assessed through four specific stages of printing, which spanned from the unprinted (Stage 1) to the printed (Stage 4) condition. Overall, the reduction in strength with respect to the unprinted filament ranged from 10 to over 60 %, with the largest degradation resulting from deposition of the filament from the nozzle onto the print bed (i.e., Stage 4). While there was no trend in strength degradation with fiber volume fraction, the largest reduction occurred to the carbon fiber filament with lowest fiber count (1k vs 6k). For the commercial materials with nylon matrix, the system with Kevlar fibers underwent less degradation in printing than that with carbon fibers. The experimental filaments with nominal volume fractions of 40 and 50 % achieved the lowest reduction in printed strength overall (as low as 10 %) and exhibited higher reliability according to a Weibull analysis. The carbon fiber system with larger V_f had a higher initial strength but lower printed strength. To increase the strength and reliability of continuous fiber composites printed by FFF and expand the potential for applications in fields involving safety-critical components, further advancements in the material and printing process are necessary.

CRediT authorship contribution statement

M. Parker: Investigation, Writing – original draft. **N. Ezeokeke:** Investigation, Visualization. **R. Matsuzaki:** Investigation, Conceptualization, Supervision. **D. Arola:** Conceptualization, Funding acquisition, Supervision.

Data availability

Data will be made available on request.

Declaration of Competing Interest

The authors declare that they have no known competing financial interests or personal relationships that could have appeared to influence the work reported in this paper: [Dwayne Arola reports a relationship with Toray Composite Materials America Inc that includes non-financial support in the form of materials donations.].

Acknowledgements

The authors acknowledge support from the Joint Center for Aerospace Technology Innovation (JCATI; PI Arola), and the National Science Foundation (N. Ezeokeke; NSF S-STEM, DUE: 1833854). Part of this work was conducted at the Molecular Analysis Facility, a National Nanotechnology Coordinated Infrastructure (NNCI) site at the University of Washington, which is supported in part by funds from the National Science Foundation (awards NNCI-2025489, NNCI-1542101), the Molecular Engineering & Sciences Institute, and the Clean Energy Institute. The authors also gratefully acknowledge Toray Industries, Inc., Japan, for their supply of materials and technical advice.

Appendix A. Supplementary material

Supplementary data to this article can be found online at https://doi.org/10.1016/j.matdes.2022.111505.

References

- [1] X. Wang, M. Jiang, Z. Zhou, J. Gou, D. Hui, 3D printing of polymer matrix composites: a review and prospective, Compos. B Eng. 110 (2017) 442–458, https://doi.org/10.1016/j.compositesb.2016.11.034.
- [2] H. Zhao, X. Liu, W. Zhao, G. Wang, B. Liu, An overview of research on FDM 3D printing process of continuous fiber reinforced composites, J. Phys. Conf. Ser. 1213 (5) (2019) 052037.
- [3] B. Brenken, E. Barocio, A. Favaloro, V. Kunc, R.B. Pipes, Fused filament fabrication of fiber-reinforced polymers: a review, Addit. Manuf. 21 (2018) 1–16, https://doi.org/10.1016/j.addma.2018.01.002.
- [4] L.G. Blok, M.L. Logana, H. Yu, B. Woods, An investigation into 3D printing of fibre reinforced thermoplastic composites, Addit. Manuf. 22 (2018) 176–186, https://doi.org/10.1016/j.addma.2018.04.039.
- [5] R. Weiss, Fabrication techniques for thermoplastic composites, Cryogenics 31 (1991) 319–322, https://doi.org/10.1016/j.addma.2018.04.039.
- [6] R. Matsuzaki, M. Ueda, M. Namiki, T.-K. Jeong, H. Asahara, K. Horiguchi, T. Nakamura, A. Todoroki, Y. Hirano, Three-dimensional printing of continuous-fiber composites by in-nozzle impregnation, Sci. Rep. 6 (2016) 23058, https://doi.org/10.1038/srep23058.
- [7] B. Akhoundi, A.H. Behravesh, A.B. Saed, Improving mechanical properties of continuous fiber-reinforced thermoplastic composites produced by FDM 3D printer, J. Reinf. Plast. Compos. 38 (2019) 99–116, https://doi.org/10.1177/ 0731684418807300.
- [8] W. Hao, Y. Liu, H. Zhou, H. Chen, D. Fang, Preparation and characterization of 3D printed continuous carbon fiber reinforced thermosetting composites, Polym. Test. 65 (2018) 29–34, https://doi.org/10.1016/j. polymertesting.2017.11.004.
- [9] A. Dickson, J. Barry, K. McDonnell, D. Dowling, Fabrication of continuous carbon, glass and Kevlar fibre reinforced polymer composites using additive manufacturing, Addit. Manuf. 16 (2017) 146–152, https://doi.org/10.1016/j. addma.2017.06.004.
- [10] P. Parandoush, D. Lin, A review on additive manufacturing of polymer-fiber composites, Compos. Struct. 182 (2017) 36–53, https://doi.org/10.1016/ j.compstruct.2017.08.088.
- [11] S.M.F. Kabir, K. Mathur, A.-F.-M. Seyam, A critical review on 3D printed continuous fiber-reinforced composites: history, mechanism, materials and properties, Compos. Struct. 232 (2020), https://doi.org/10.1016/ i.compstruct.2019.111476 111476.
- [12] A. Khudiakova, M. Berer, S. Niedermair, B. Plank, E. Truszkiewicz, G. Meier, H. Stepanovsky, M. Wolfahrt, G. Pinter, J. Lackner, Systematic analysis of the mechanical anisotropy of fibre-reinforced polymer specimens produced by laser sintering, Additive Manuf. 36 (2020), https://doi.org/10.1016/j.addma.2020.101671 101671.

- [13] H.L. Tekinalp, V. Kunc, G.M. Velez-Garcia, C.E. Duty, L.J. Love, A.K. Naskar, C.A. Blue, S. Ozcan, Highly oriented carbon fiber-polymer composites via additive manufacturing, Compos. Sci. Technol. 105 (2014) 144–150, https://doi.org/ 10.1016/j.compscitech.2014.10.009.
- [14] N.M. DeNardo, Additive manufacturing of carbon fiber-reinforced thermoplastic composites, Open Access These. 939 (2016). https://docs.lib. purdue.edu/open_access_theses/939.
- [15] X. Tian, A. Todoroki, T. Liu, L. Wu, Z. Hou, M. Ueda, Y. Hirano, R. Matsuzaki, K. lizuka, A.V. Malkhov, A.N. Polilov, D. Li, B. Lu, 3D Printing of continuous fiber reinforced polymer composites: development, application, and prospective, chinese journal of mechanical engineering: additive manufacturing, Frontiers. 1 (2022), https://doi.org/10.1016/j.cjmeam.2022.100016 100016.
- [16] H. Zhang, J. Wu, C. Robert, C.M.Ó. Brádaigh, D. Yang, 3D printing and epoxy-infusion treatment of curved continuous carbon fibre reinforced dual-polymer composites, Compos. B Eng. 234 (2022), https://doi.org/10.1016/j.compositesb.2022.109687 109687.
- [17] X. Tian, T. Liu, C. Yang, Q. Wang, D. Li, Interface and performance of 3D printed continuous carbon fiber reinforced PLA composites, Compos. A Appl. Sci. Manuf. 88 (2016) 198–205, https://doi.org/10.1016/ j.compositesa.2016.05.032.
- [18] Y. Hu, R.B. Ladani, B. Milan, L. Yazhi, A.P. Mouritz, Carbon fibre damage during 3D printing of polymer matrix laminates using the FDM process, Mater. Des. 205 (2021), https://doi.org/10.1016/j.matdes.2021.109679 109679.
- [19] Z. Zhang, Y. Long, Z. Yang, K. Fu, Y. Li, An investigation into printing pressure of 3D printed continuous carbon fiber reinforced composites, Compos. A Appl. Sci. Manuf. 162 (2022), https://doi.org/10.1016/j.compositesa.2022.107162 107162.
- [20] M. Parker, A. Inthavong, E. Law, S. Waddell, N. Ezeokeke, R. Matsuzaki, D. Arola, 3D printing of continuous carbon fiber reinforced polyphenylene sulfide: exploring printability and importance of fiber volume fraction, Addit. Manuf. 54 (2022), https://doi.org/10.1016/j.addma.2022.102763 102763.
- [21] P. Zhuo, S. Li, İ.A. Ashcroft, I.A. Jones, Continuous fibre composite 3D printing with pultruded carbon/PA6 commingled fibres: processing and mechanical properties, Compos. Sci. Technol. 221 (2022), https://doi.org/10.1016/ j.compscitech.2022.109341 109341.
- [22] P. Vasanthakumar, K. Sekar, K. Venkatesh, Recent developments in powder metallurgy based aluminium alloy composite for aerospace applications, Mater. Today:. Proc. 18 (2019) 5400–5409, https://doi.org/10.1016/ j.matpr.2019.07.568.
- [23] S. Mabuwa, V. Msomi, M. Oritanda, S.M. Sharon, The microstructure and mechanical properties of the friction stir processed TIG-welded aerospace dissimilar aluminium alloys, Mater. Today:. Proc. 46 (2021) 658–664, https:// doi.org/10.1016/j.matpr.2020.11.588.
- [24] P. Pushp, S.M. Dasharath, C. Arati, Classification and applications of titanium and its alloys, Mater. Today:. Proc. 54 (2022) 537–542, https://doi.org/ 10.1016/j.matpr.2022.01.008.
- [25] T.S. Tshephe, S.O. Akinwamide, E. Olevsky, Additive manufacturing of titanium-based alloys- A review of methods, properties, challenges, and prospects, Heliyon. 8 (2022) e09041, https://doi.org/10.1016/j.heliyon.2022.
- [26] D. Jang, M.E. Lee, J. Choi, S.Y. Cho, S. Lee, Strategies for the production of PAN-Based carbon fibers with high tensile strength, Carbon 186 (2022) 644–677, https://doi.org/10.1016/j.carbon.2021.10.061.
- [27] O. Benjeddou, Weibull statistical analysis and experimental investigation of size effects on tensile behavior of dry unidirectional carbon fiber sheets, Polym. Test. 86 (2020), https://doi.org/10.1016/j.polymertesting.2020.106498 106498.
- [28] Y. Swolfs, I. Verpoest, L. Gorbatikh, Issues in strength models for unidirectional fibre-reinforced composites related to Weibull distributions, fibre packings and boundary effects, Compos. Sci. Technol. 114 (2015) 42–49, https://doi.org/ 10.1016/j.compscitech.2015.04.002.
- [29] K. Naito, Y. Tanaka, J.M. Yang, Y. Kagawa, Tensile properties of ultrahigh strength PAN-based, ultrahigh modulus pitch-based and high ductility pitchbased carbon fibers, Carbon 46 (2008) 189–195, https://doi.org/10.1016/ icarbon.2007.11.001.
- [30] D. Loidl, O. Paris, H. Rennhofer, M. Müller, H. Peterlik, Skin-core structure and bimodal Weibull distribution of the strength of carbon fibers, Carbon 45 (2007) 2801–2805, https://doi.org/10.1016/j.carbon.2007.09.011.
- [31] S.K. Paul, A. Nayak Majila, D.C. Fernando, Statistical analysis of uniaxial tensile and fatigue data of Ti-685 alloy at different temperatures, Forces in Mechan. 4 (2021), https://doi.org/10.1016/j.finmec.2021.100046 100046.
- [32] A.H. Shevidi, R. Taghiabadi, A. Razaghian, Weibull analysis of effect of T6 heat treatment on fracture strength of AM60B magnesium alloy, Trans. Nonferrous Met. Soc. Chin. 28 (2018) 20–29, https://doi.org/10.1016/S1003-6326(18) 64634-5.
- [33] B.G. Eisaabadi, P. Davami, S.K. Kim, M. Tiryankioğlu, The effect of melt quality and filtering on the Weibull distributions of tensile properties in Al-7%Si-Mg alloy castings, Mater. Sci. Eng. A 579 (2013) 64-70, https://doi.org/10.1016/j. msea.2013.05.014.
- [34] J. Justo, L. Távara, L. Garcia-Guzmán, F. Paris, Characterization of 3D printed long fibre reinforced composites, Compos. Struct. 185 (2018) 537–548, https://doi.org/10.1016/j.compstruct.2017.11.052.
- [35] F. van der Klift, Y. Koga, A. Todoroki, M. Ueda, Y. Hirano, R. Matsuzaki, 3D Printing of Continuous Carbon Fibre Reinforced Thermo-Plastic (CFRTP) Tensile Test Specimens, Open, J. Compos. Mater. 6 (2016) 18–27, https://doi. org/10.4236/ojcm.2016.61003.

- [36] M. Heidari-Rarani, M. Rafiee-Afarani, A.M. Zahedi, Mechanical characterization of FDM 3D printing of continuous carbon fiber reinforced PLA composites, Compos. B Eng. 175 (2019), https://doi.org/10.1016/j.compositesb.2019.107147 107147.

 [37] X. Peng, M. Zhang, Z. Guo, S. Lin, W. Hou, Investigation of processing parameters on tensile performance for FDM-printed carbon fiber reinforced
- polyamide 6 composites, Compos. Commun. 22 (2020) 1000478, https://doi.
- org/10.1016/j.coco.2020.100478.

 [38] R. Shuto, S. Norimatsu, D. Arola, R. Matsuzaki, Effect of the nozzle temperature on the microstructure and interlaminar strength in 3D printing of carbon fiber/PPS composites, Composites: C. (2022). in press.